International Journal of Theoretical and Applied Research (IJTAR)
ISSN: 2812-5878

Homepage: https://ijtar.journals.ekb.eg

Original article

Valorization of Lemon Peel as a low-cost adsorbent for the removal of Basic Fuchsine and Eosin dyes from aqueous solutions

Nada M. Sayed [1*], Gamalat Al-Mohamady [1], Samia A. Abo-Farha [1], Nagwa A. Badawy [1], Mahmoud O. El-Moatasem [2]

[1] *Faculty of Science, Al-Azhar University (Girls Branch), Cairo, Egypt.*
[2] *Faculty of Agriculture, Al-Azhar University (Male Branch), Cairo, Egypt.*

ARTICLE INFO

Received 06/04/2023
Revised 12/06/2023
Accepted 25/06/2023

Keywords

Wastewater
Basic fuchsine
Eosin
Lemon peel
Kinetics
Isotherms
Thrmodynamics

ABSTRACT

The objective of this study was to investigate the potential of natural wastes (lemon peel) as an adsorbent for the removal of Basic Fuchsine (BF) and Eosin (E) dyes from effluents. Lemon peel was used in inactivated (IALP) and activated (ALP) forms. Both were characterized using FTIR and SEM analysis. The lemon peel was washed, treated with H_3PO_4, and then heated to 120°C. Parameters like pH, adsorbent dose and size, initial dye concentration, contact time, and temperature were studied. A pseudo-second-order kinetic model provides the best fit to the experimental data according to R^2 values. The maximum adsorption capacities were 1.5133, 1.8142 $mg.g^{-1}$ for BF adsorption, and 1.2393, 1.5974 $mg.g^{-1}$ for E adsorption, onto IALP and ALP respectively according to pseudo-second-order kinetic model. This indicates the formation of dyes monolayer onto the lemon peel surface. Maximum adsorption capacities were calculated from the Langmuir model to be 3.0731, 3.3190 $mg.g^{-1}$ for BF adsorption, and 3.1646, 4.0388 $mg.g^{-1}$ for E adsorption onto IALP and ALP respectively. The values of R_L according to the Langmuir model and n according to the Freundlich model indicate that the adsorbate is favorably adsorbed on the adsorbent. The mean free energy per molecule of adsorbate E was ranging from 0.1291 to 5.00 $kJ{\cdot}mol^{-1}$ which indicates that the adsorption is controlled by physical process. The activation parameters (ΔG^o, ΔH^o, ΔS^o) were calculated. The adsorption was endothermic, and spontaneous with a high preference of dyes onto IALP and ALP.

Graphical abstract

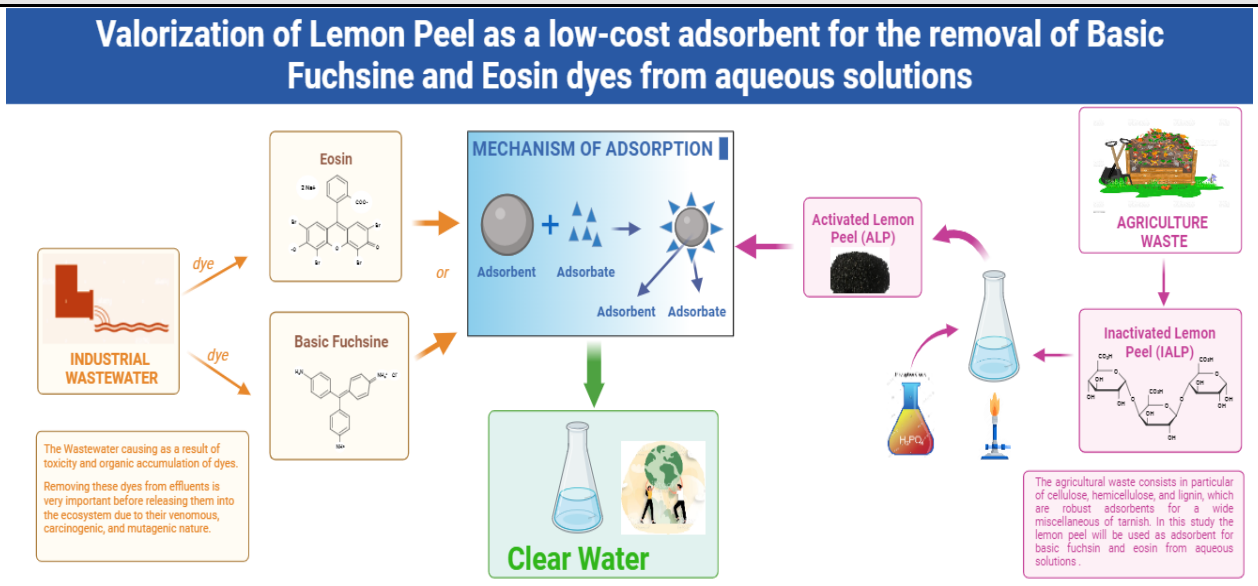

* *Corresponding author*
E-mail address: chem.nada.sayed@gmail.com

DOI: 10.21608/IJTAR.2023.197859.1041

1. Introduction

Presently, considering the rapid development of industrialization and urbanization activities, a massive quantity of wastewater is generated [1]. Aqueous system pollution comes for several reasons, one of the most important of which is textile wastewater which is caused as a result of toxicity and organic accumulation of dyes [2]. Removing these dyes from effluents is very important before releasing them into the ecosystem due to their venomous, carcinogenic, and mutagenic nature [3]. The main five resources of dye effluent pollution are the textile (54%), dyeing (21%), paper and pulp (10%), tannery and paint industry (8%), and dye manufacturing industry (7%) [4]. There are many physical, chemical, and biological ways to sweep dyes [5] like photocatalytic, oxidation, membrane filtration, flocculation, precipitation, and biodegradable or adsorption processes [6,7].

Wastewater remediation plants seldom use sophisticated treatment with regard to their price. Adsorption is a rifer method due to its affordability, security, and opportunity for sorbent renovation [8]. The agricultural waste consists in particular of cellulose, hemicellulose, and lignin, which are robust adsorbents for a wide miscellaneous of tarnish because of the presence of functional groups like hydroxylic and carboxylic phenols. They have a high adsorption rate and selection for diverse impurities and can be used with and without minimal treatment [9]. These natural adsorbents are perfect due to their availability in huge quantities requiring a simple preparation to strengthen the benefits of the adsorption processes, in agreement with the perceptions of green chemistry [10]. They can be considered very effective for their low cost, and high efficiency, can be used at a wide pH range [11], and it is possible to recover the adsorbate, as well as the ability to reproduce natural adsorbent [12]. On the other hand, the limitation of using natural products are mainly about the adsorbent recovery and separation after treatment [13]. In the current work, lemon peel is used as a natural adsorbent which is available locally in Egypt. It is used in two forms inactive lemon peel (IALP) and activated lemon peel (ALP).

The activated lemon peel is obtained by using H3PO4 and the resulting activated carbon is then used in batch adsorption of basic Fuchsine (BF) and Eosin (E) [14]. The structural classification of dyes can be determined by their functional groups, in this study, basic Fuchsine (BF) and Eosin (E) were used as two examples for basic and acid dyes respectively [15]. Basic Fuchsine, named Basic Violet 14, which is scientifically named benzenamine, 4-[(4-aminophenyl) (4-imino-2, 5-cyclohexadien-1-ylidene) methyl]-2-methyl hydrochloride, Fig. 1 [16]. Eosin also known as Acid Red 87, is chemically known as disodium; 2-(2,4,5,7-tetrabromo-3-oxido-6-oxoxanthen-9-yl) benzoate, Fig. 2. Both of them are widely employed in tapestry, meds preparations, and manufacturing [17].

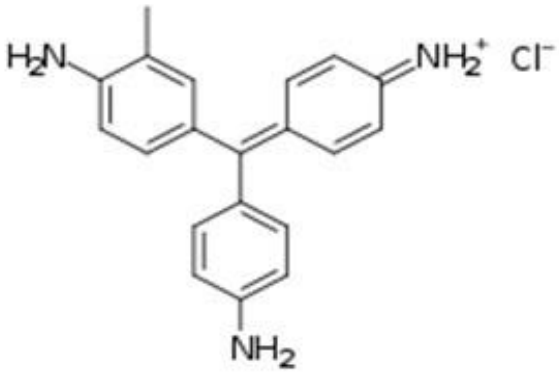

Fig. 1 Chemical structure of Basic Fuchsine.

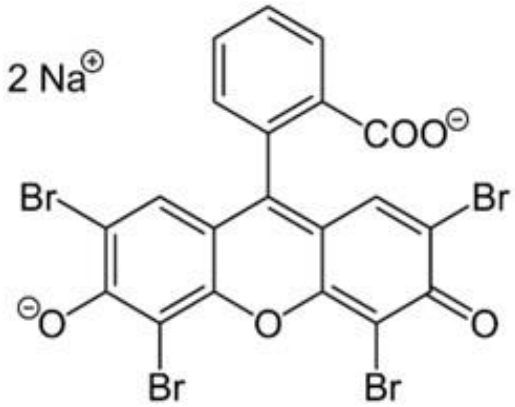

Fig. 2 Chemical structure of Eosin.

2. Materials and methods

2.1. Materials

Lemon is a local product grown abundantly in Egypt. Basic Fuchsine (BF) and Eosin (E) dyes were made in India (Advent, Chembio PVT.LTD company) and purchased from Maktab Al-Sharq, Qasr El-Ainy, Cairo, Egypt. The dye's maximum wavelengths, also molar masses are depicted in Table 1. The chemical compounds: sodium hydroxide (NaOH), hydrochloric (HCl), and phosphoric acids (H3PO4) were also purchased from Maktab Al-Sharq.

Table 1 Dyes mol. wt. and λ_{max}

Dye name	Basic Fuchsine	Eosin
Molecular weight (mol. wt.)	337.86 g/mol	691.85 g/mol
Maximum wavelength (λ_{max})	546 nm	514 nm

The functional groups' declaration in both adsorbents IALP and ALP which may work as active sites during the adsorption process is achieved via using Fourier Transform Infrared Spectroscopy analysis [18].

The morphological properties and microstructure of both adsorbents were investigated using a Scanning Electron Microscope model [19].

Batch adsorption tests were established for studying various impacts on the sorption. Adsorption kinetics in addition to isotherms were studied and thermodynamic parameters were calculated.

2.2. Preparation of adsorbents

The To prepare the inactive lemon peel adsorbent (IALP), the lemon peels were washed multiple times to dismantle impurities, color, and odor, then dehydrated for 24 hr. at a temperature of 50°C using a drying oven. Then they were crushed into two particle sizes (0.1 mm and 0.2mm). This adsorbent was used to prepare the activated lemon peel adsorbent (ALP) [20]. A solution of 50 ml, 0.6 M phosphoric acid was mixed with 2g of IALP at room temperature and stirred for 30 minutes, then centrifuged and dehydrated at 50°C for 24 hr. The thermostat then has been increased to 120°C for 90 minutes. The obtained adsorbent then was washed numerous times to remove the undue acid. Then it has been allowed to dry at 50°C for 24 hr. The ALP has been crushed into two particle sizes (0.1 mm and 0.2mm) [21].

2.3. Adsorption study

Batch tests were implemented using 50 ml of dye solution and the percentage of removal was studied with the change of several factors. The tests were executed at differing pH (3-11), different adsorbent doses (0.4, 0.8, 1.2, 1.6, and 2 g), different dye concentrations (35, 70, 100, 135, 170, 200, 235, 270, 300, 335 mg.l-1), particle sizes (0.1 and 0.2 mm), contact time (from 5 to 180 min) and different temperatures (298, 323 and 343 K) at 200 rpm.

Using Equations 1 and 2 gives the efficiency and capacity of adsorption [22].

$$\text{Removal efficiency } (\%) = \frac{Co-Ce}{Co} \times 100 \qquad [1]$$

$$q\ (mg/g) = \frac{(Co-Ce)xV}{m} \qquad [2]$$

The dye concentrations were determined precisely by UV/VIS Spectrometer [23,24].

3. Results and Discussion

3.1. Characterization of adsorbents

3.1.1. Fourier transform infrared

This analysis helps in giving an elaborate view of the function groups and the change in them via activation and adsorption [25]. The main plugs of lemon peel are protein, pectin, cellulose, hemicellulose, lignin, and pigments. This analysis is crucial to feature the interactive functional sets which contain various giving atoms such as O, N, S, and P [26]. Fig. 3 shows the FTIR spectrum of lemon peel (a), activated lemon peel (b), activated lemon peel with basic fuchsin dye (c), and activated lemon peel with eosin dye (c). The large peaks at 3200 – 3424 cm–1 is representing the symmetric and asymmetric stretching vibrations of free or H-bonded hydroxyl groups of phenols, alcohols, and carboxylic acids contained in cellulose, pectin, and lignin [27]. The values around 2924 cm^{-1} represent the symmetric and asymmetric stretching vibrations of the -CH_3, =CH_2, and -OCH_3 groups [26].

The next peak at 1734.58 cm–1 for IALP may correspond to stretching vibrations of the ester carbonyl C=O group. This peak disappeared as a finding of the adsorption and was not noticed in the (c) and (d) figures. The peak of 1627.45 cm-1 represents –C≡C– stretch and alkanes. The following peak is 1381.84 cm-1 which has C–H rock and is alkane [28]. The other one around 1623 cm–1 was a mark of stretching vibration of carboxylate ions COO-1. The other peaks in the range of 1300 – 1020 cm–1 could be owing to the compounds containing a C-O group which may be Alcohols, carboxylic acids, esters, or ethers [28,29]. The spectra of ALP-loaded BF and E dyes showed similar characteristics of adsorption regions except for minor changes and the peaks are a bit shifted from their sites with changes in its intensity. The hydrogen bonding, electrostatic, and π -π interactions carry out the adsorption processes [18,30].

3.1.2. Scan electron microscope

Figure (4) shows the SEM analysis before and after the activation and the adsorption processes with BF and E dyes. It is clear that there is a significant change after the adsorption. The adsorbent surfaces are conquered, and sorbate particles subsume the surface follicles [28]. The use of H3PO4 for activation increases the pore size allocation of lemon peel and therefore the adsorption potential [31].

The shape of the lemon peel surface, as shown in the image, was found to possess irregular and heterogeneous active sites which were unevenly distributed. The normal lemon peel was changed to an excellent porous material, as a result of the activation process. It looked like regular homogenous creases spanned the surface.

This structure permits powerful adsorption because it introduces sufficient free areas to seek adsorbate particles [32].

It is clear, by comparing Figures a and b, that there was an excess in the pore size distribution of activated lemon peel. The activated surface has a shape similar to a honeycomb and the spacious murk spots are pores and vacuums on its surface [33].

Figures (c) and (d) represented the occupation of Basic Fuchsine and Eosin molecules, which were investigated through the thickened and enclosed pores.

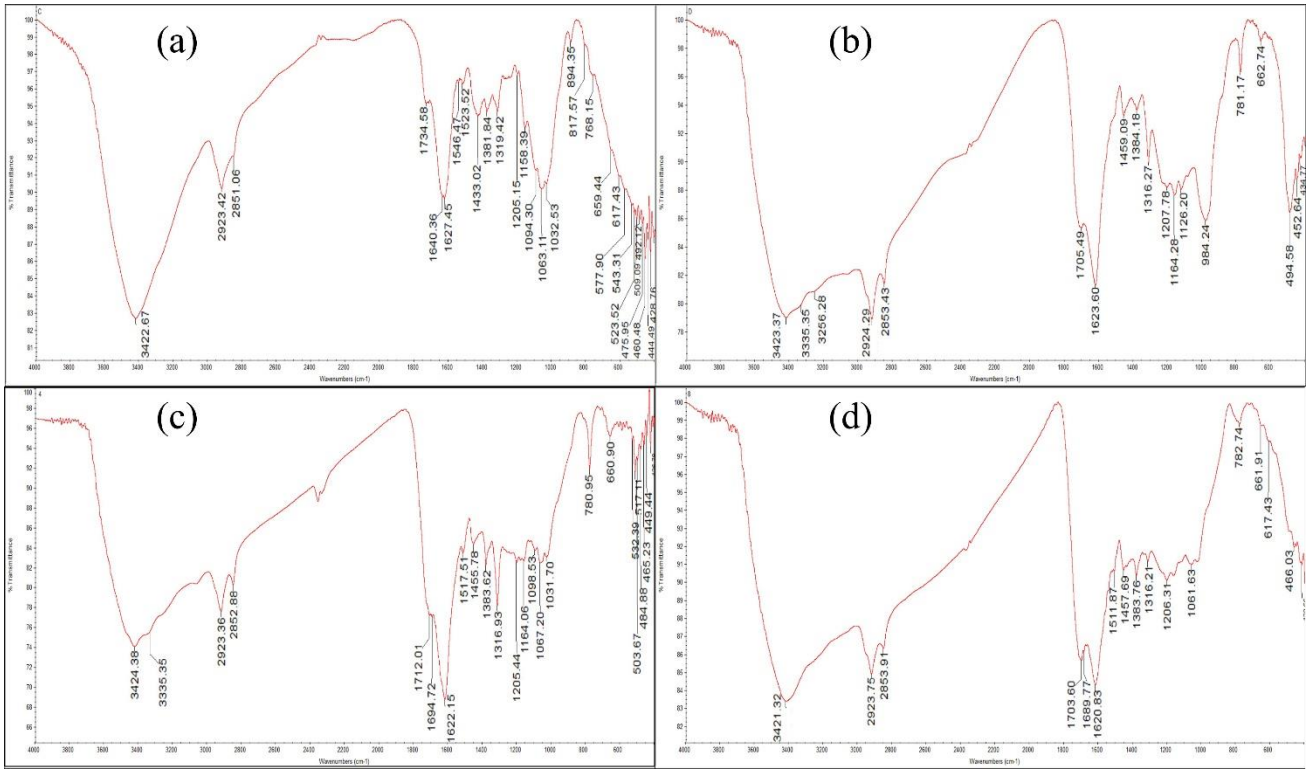

Fig. 3 FTIR spectrum. (a) IALP, (b) ALP, (c) BF onto ALP, (d) E onto ALP.

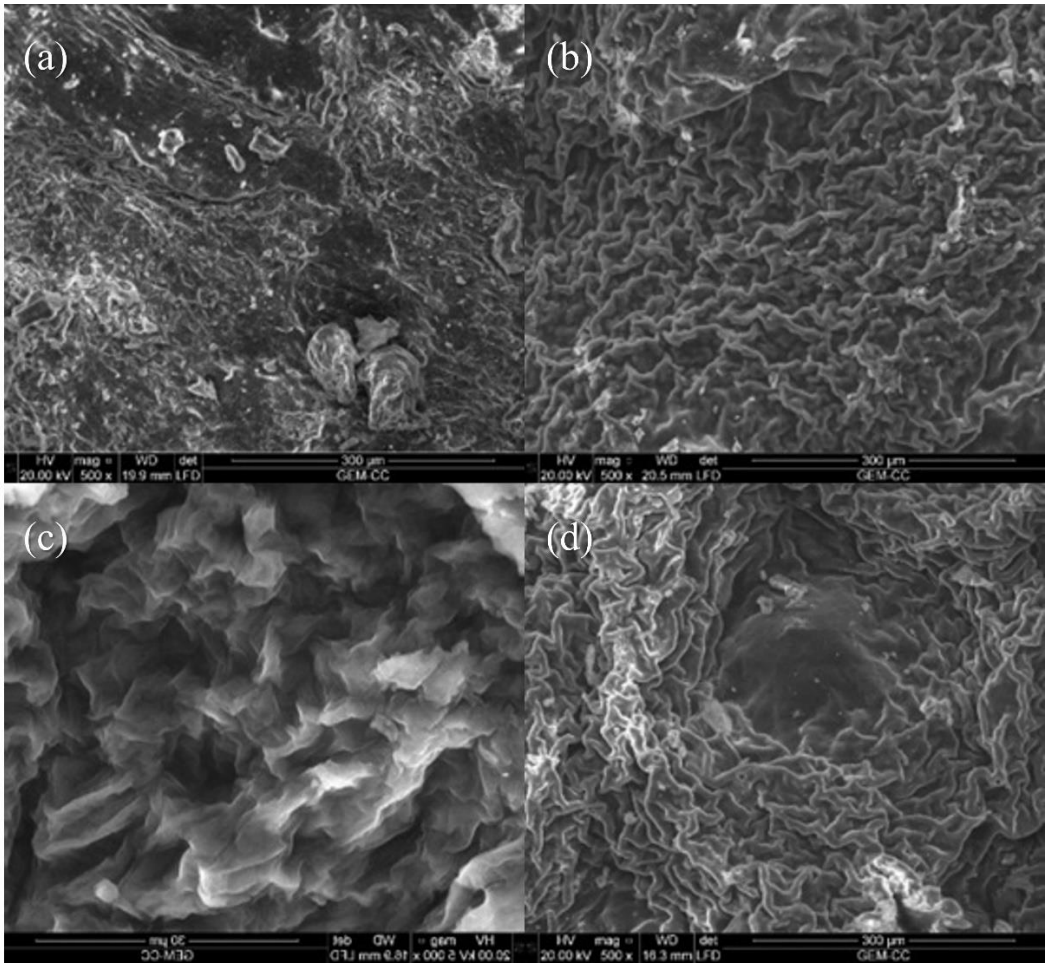

Fig. 4 SEM micrograph. (a) IALP, (b) ALP, (c) BF onto ALP, (d) E onto ALP.

3.2. Impact of pH

The pH impact on the adsorption is due to the fact that the surface properties of adsorbent and ionization grade of adsorbate vary with pH [34]. The conditions of the experiments were a volume of 50 ml solution, 35 $mg.l^{-1}$ dye concentration, 2 g adsorbent dose of 0.1 mm particle size, 200 rpm at room temperature and for 180 minutes. It was found that by changing the values of pH from 3 to 11, we get maximum removal values of 69.25% and 90.52% for E dye onto IALP and ALP respectively at pH3. And we get maximum removal values of 86.17% and 99.94% for BF dye onto IALP and ALP respectively at pH11. This is explained as at pH3 the surfaces of IALP and ALP were positively charged and elevation of protons number will occur which will be accessed for amine points, and this increases the active sites and thus prefer anion sorption resulting in increasing the removal of E. While at superior pH, most of the active sites preferred for E dye may be separated and cause a shortfall in adsorption gage [35]. On the other hand, at pH11 the surface charges of IALP and ALP are adverse and firmly grabbed to favorably BF ions. While within acid solutions, a challenge among extra H+ ions and the positive BF ions towards the active locations on the adsorbent surfaces occurs and leads to a shortfall in adsorption capabilities onto IALP and ALP [36]. The results are presented in Fig. 5.

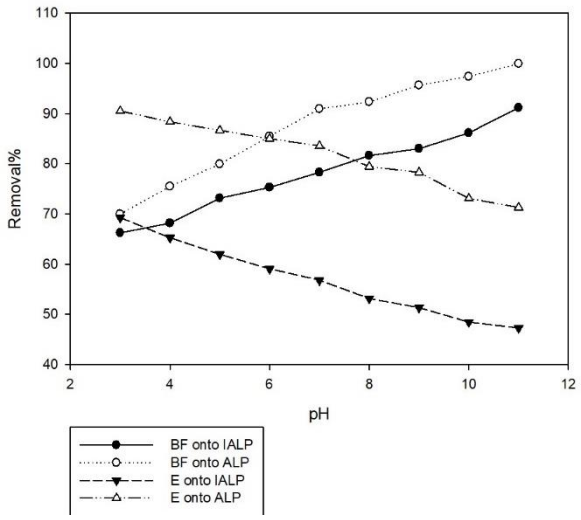

Fig. 5 Impact of pH.

3.3. Impact of adsorbent quantity and particle size

This impact was studied under the conditions of 50 ml solution volume, 35 $mg.l^{-1}$ primary dye concentration, pH11 and pH3 for BF dye and E dye respectively, at 200 rpm at room temperature and for 180 minutes. It was found that by raising the dose values of both IALP and ALP adsorbents from 0.4 to 2 g, the adsorption grows for both dyes due to the greater area accessible for the process [37], this is presented in Fig. 6.

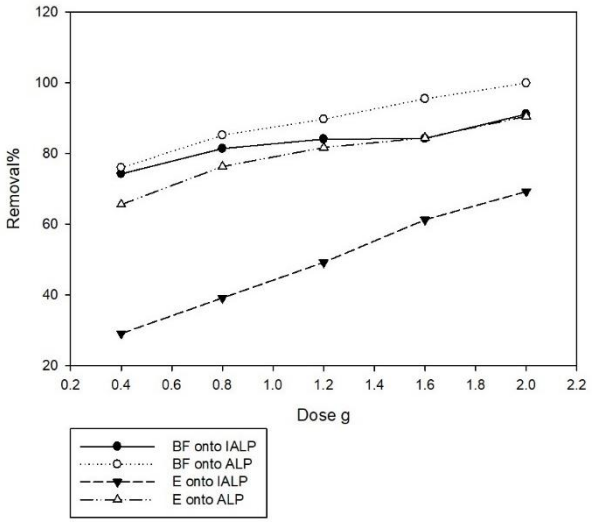

Fig. 6 Impact of adsorbent dose.

On the other hand, declining the particle size from 0.2 to 0.1 mm increases the capacity of the adsorption, this is because of the fact that a small particle has a broader surface area and the amount of dye adsorbed is directly proportional to the volume of the pores, which is directly proportional to the external interfacing area of adsorbent particles [38]. This is presented in Fig. 7.

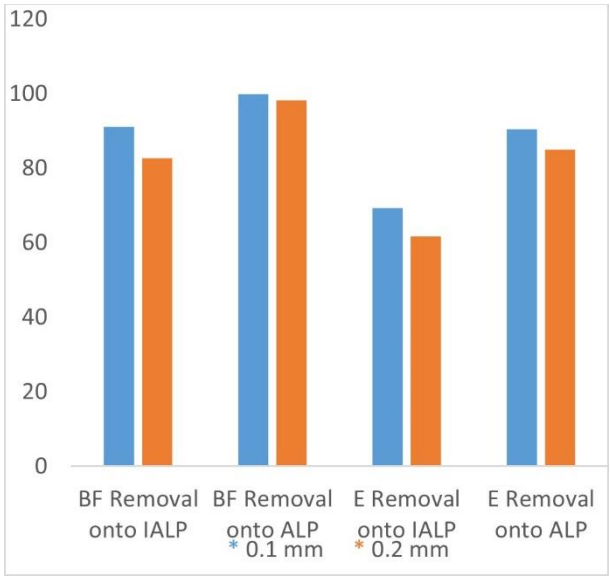

Fig. 7 Impact of adsorbent particle size.

3.4. Impact of primary dye concentration

This impact was examined under the terms of 50 ml dye solution, 2 g of adsorbents, pH11 and pH3 for BF and E dyes respectively, at 200rpm and for 240 minutes at room temperature with a primary concentration scale within 35 to 335 $mg.l^{-1}$. It was found that by increasing the primary concentration for both dyes, the adsorption minimizes onto both adsorbents IALP and ALP. The removal dropped from 86.17% to 40.29% and from 99.94% to 59.54% for BF adsorption and dropped from 69.25% to 29.59% and from 90.52% to 45.71% for adsorption of E dye onto IALP and ALP respectively.

From experimental results, it was found also that ALP and IALP have a stronger convergence toward BF dye than E dye, and in general, ALP showed better results than IALP because of the activation process. The decrease in dye removal by increasing their primary concentrations is because of the high ratio of dye primary concentration in comparison with the existing active points so the process is affected by the starting concentration [39]. The results are presented in Fig. 8.

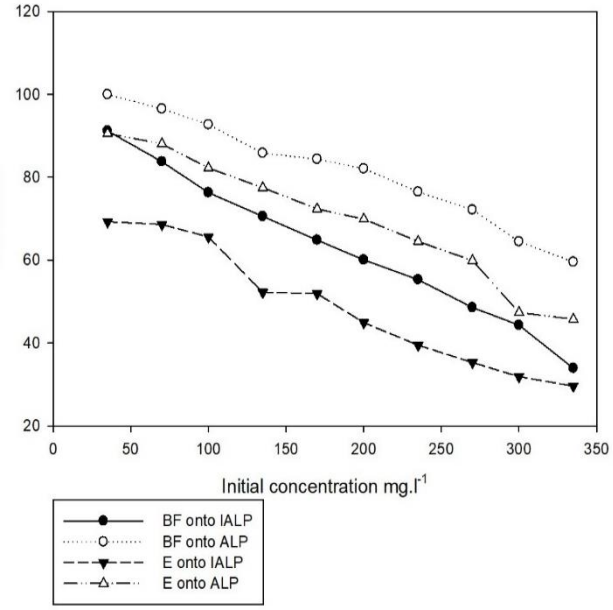

Fig. 8 Impact of initial dye concentration.

3.5. Impact of contact time

This impact was studied under the optimum conditions which were obtained from previous experiments for 180 minutes and the equilibrium time was found to be 35 min. and 30 min. for BF dye onto IALP and ALP respectively and was found to be 40 min. and 25 min. for E dye onto IALP and ALP respectively.

It is of economic importance to target adequate contact time to achieve the removal purpose. It was observed that it was a sharp exceed in adsorption for a small period thereafter the equilibrium is reached no splendid adsorption is observed. After reaching the equilibrium, the repulsive electrostatic interaction will be dominant between the occupied active sites and the adsorbate particles [40]. The results are presented in Fig. 9.

3.6. Impact of temperature

The impact of temperature was studied under the optimum conditions at temperatures 298, 323, and 343 K. There was an improvement in dye removal by raising the temperature is attributed to the higher mobility and proliferation of the ionic dye molecules in solution at higher temperature values [41].

From the experimental data, it was found that the value of adsorption increasing by increasing temperature was not very high, so the adsorption process for BF and E dyes onto ALP did not require heating to give high removal values. This makes the clearance of dyes may be accomplished onto ALP economically and has artificial applications [42]. The results are presented in Fig. 10.

According to the maximum removal percentages at the optimum conditions, it can be concluded that IALP at an acidic medium was positively charged and can attract negatively charged E dye better than the positively charged BF. While, in the alkaline medium the opposite behavior was occurring. After activation with acidic H_3PO_4 and heating, the resulting ALP was an effective adsorbent because it is a highly porous material and provides a large surface area to which contaminants may adsorb [43].

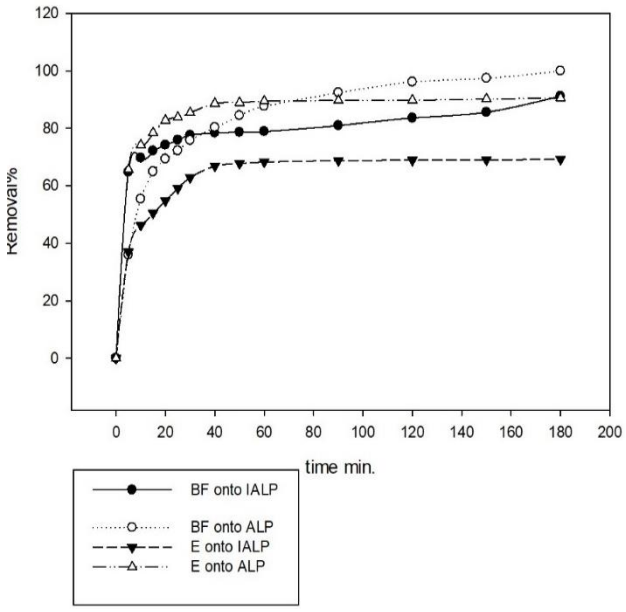

Fig. 9 Impact of contact time.

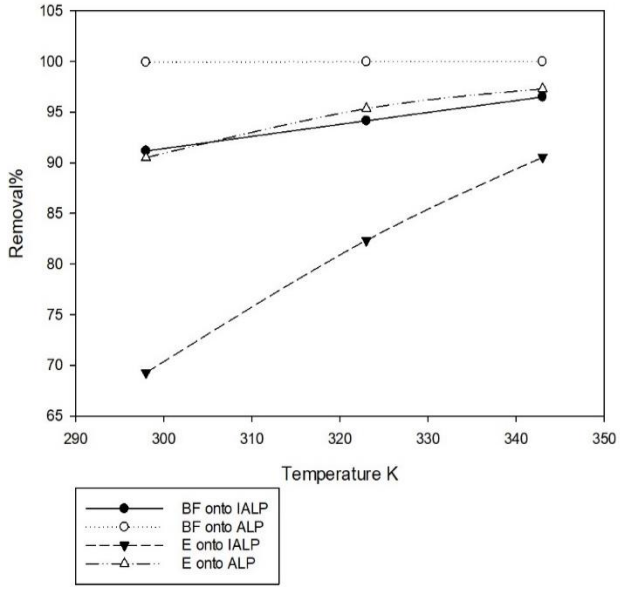

Fig. 10 Impact of temperature.

3.7. Adsorption models

3.7.1. Adsorption kinetics

The experiments were executed using 50 ml solutions of primary BF and E concentrations 35 $mg.l^{-1}$ at optimum conditions of pH 11 and pH3 for BF and E respectively, adsorbents (IALP and ALP) doses of 2 g with 0.1 mm particle size at room temperature and for 180 minutes. Some kinetic models were used, pseudo-first-order, pseudo-second-order, intraparticle diffusion, and Elovich models [44].

3.7.1.1. The pseudo-first-order kinetic model

That model studied the alteration average of the sucking adsorbate at a certain time, which is directly proportional to the difference between the concentration and adsorbate removal rate [45,46].

This introduces the adsorption rate constant by applying Equations 3[47,48].

$$\log (q_e - q_t) = \log (q_e) - \frac{K1}{2.303} t \qquad [3]$$

The results are presented in Fig.11.

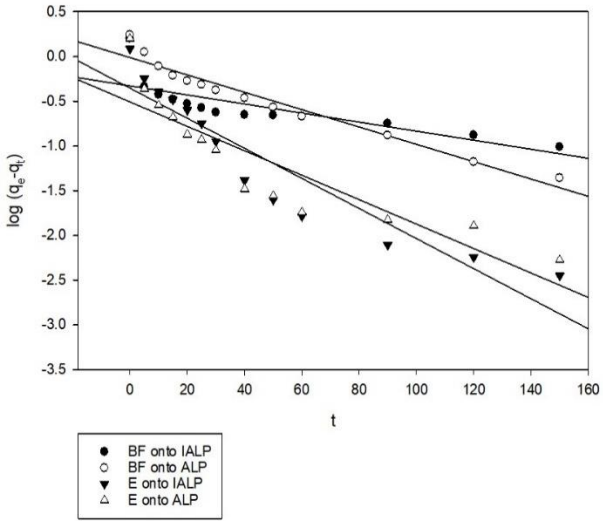

Fig. 11 Pseudo-first-order kinetic model.

3.7.1.2. The pseudo-second-order kinetic model

This model considered a chemical bonding (interaction) of adsorbate and technical points on an adsorbent surface which is responsible for the adsorption capabilities of the adsorbent [49,50]

The rate constant is estimated by applying Equation 4 [51].

$$\frac{t}{q_t} = \frac{1}{K_2\, qe^2} + \frac{t}{q_e} \qquad [4]$$

The results are presented in Fig.12.

3.7.1.3. Fourier transform infrared The intraparticle diffusion model

Can be referred to by Equation 5.

$$q_t = k_{id}.t^{1/2} + C \qquad [5]$$

If the plot goes by the origin, then intraparticle diffusion is the rate-controlling step of adsorption. If this does not occur, there is a boundary control to some extent and other kinetic models may operate the rate of the process. Experimental plots usually are shown as three phases such as curve, linear, and plateau turn. External mass transfer is represented by the primary stage. The intraparticle diffusion is represented by the intermediate linear stage. And finally, the extremely low solute concentrations in the solution will result in slowing the intraparticle diffusion and this is represented by the last plateau stage [51]. The results are presented in Fig.13.

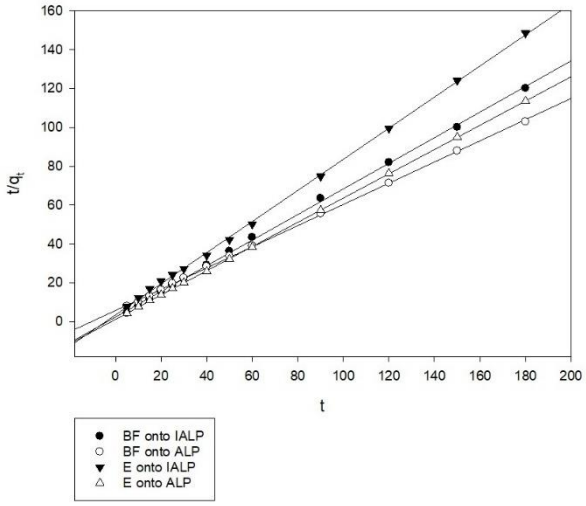

Fig. 12 Pseudo-second-order kinetic model.

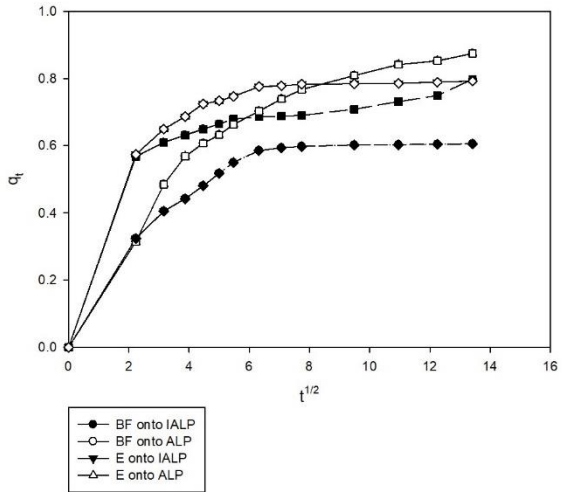

Fig. 13 Intraparticle diffusion kinetic model.

3.7.1.4. Elovich model

This model assumed that the energy of adsorbent active sites is heterogeneous and the adsorption follows a second-order kinetic model, so according to this model, the adsorption mechanism is based on chemical reactions [53].

This model can be characterized by applying the linear form of Equation 6 [54].

$$q_t = (1/\beta) \ln t + (1/\beta) \ln \alpha\beta \qquad [6]$$

The results are presented in Fig.14, the parameters are calculated and compared in Table 2.

Table 2 Kinetic parameters for BF and E dyes adsorption onto IALP & ALP

Parameter	BF onto IALP	BF onto ALP	E onto IALP	E onto ALP
Pseudo-first order kinetic model				
K1	0.0051	0.0097	0.0168	0.0137
qe	0.4701	0.9750	0.4435	0.3115
R2	0.6438	0.9531	0.8793	0.7974
Pseudo-second order kinetic model				
K2	0.1790	0.5758	0.1792	0.3118
qe	1.5133	1.8142	1.2393	1.5974
R2	0.9993	0.9995	0.9995	1
Intraparticle diffusion kinetic model				
Kid	0.0163	0.0417	0.0212	0.0148
C	0.5665	0.3881	0.3822	0.6344
R2	0.9229	0.8378	0.6684	0.6304
Elovich kinetic model				
α	1.6328	0.7847	3.3587	1.4936
β	4.1701	3.3967	6.3012	8.8968
R2	0.7411	0.9707	0.8660	0.8425

The findings demonstrated that an increase in contact between solid and liquid phases increases the adsorption. The maximum capacity of adsorption is 1.5133, 1.8142 $mg.g^{-1}$ for BF dye adsorption, and 1.2393, 1.5974 $mg.g^{-1}$ for E dye adsorption onto IALP and ALP respectively. Also, we can see from Table 2 that according to higher correlation coefficient (R^2) numbers, the adsorptions of BF and E dyes onto both IALP and ALP are better characterized by the Pseudo-second order model.

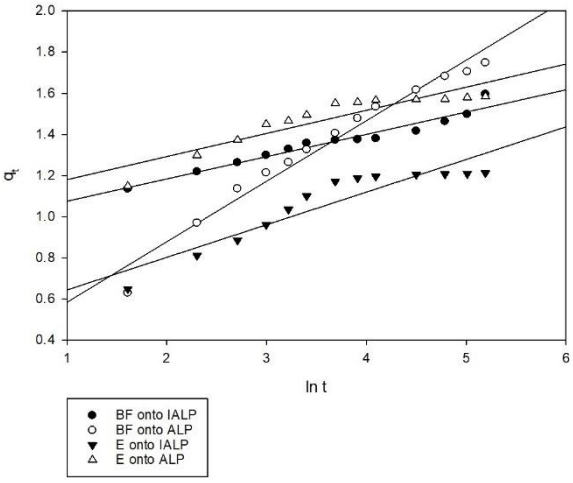

Fig. 14 Elovich kinetic model.

3.7.2. Adsorption isotherm

Adsorption isotherm expresses the relation, at a constant temperature, between adsorbed sorbate intake on the adsorbent surface to the concentration of solute when equilibrium is reached. The adsorption isotherm models are models that illustrate this correlation [55].

3.7.2.1. Langmuir isotherm model

This traditionally known isotherm presumed that adsorption takes place at certain harmonious adsorbent surfaces [56]. When the active site is occupied by an adsorbed molecule, no further adsorption will occur [57]. Accordingly reaching the equilibrium and the imbued monolayer formation be expressed by the following Equation 7 [58].

$$\frac{c_e}{q_e} = \frac{c_e}{q_o} + \frac{1}{b q_o} \qquad [7]$$

The separation factor R_L is a dimensionless constant. It predicts whether the adsorption was favorable or unfavorable in terms of equilibrium parameters [59]. It can be calculated from Equation 8.

$$R_L = \frac{1}{(1 + b C_0)} \qquad [8]$$

The values of R_L indicate whether the isotherm is unfavorable ($R_L > 1$), linear ($R_L = 1$), favorable ($R_L < 1$), or irreversible ($R_L = 0$). The results are presented in Fig.15.

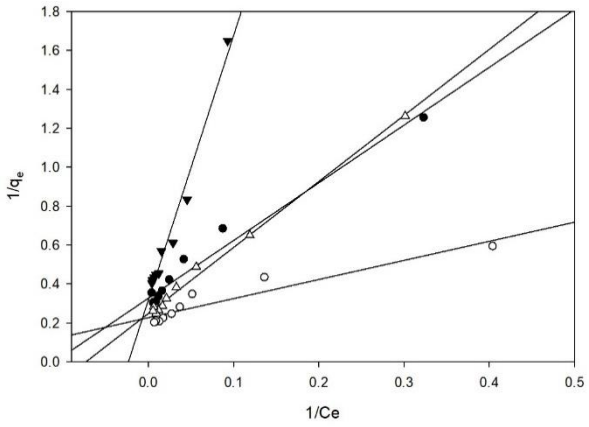

Fig. 15 Langmuir isotherm model

3.7.2.2. Freundlich isotherm model

That model depicts the adsorption process as it takes place across heterogeneous roof top and the multilayer adsorption system is considered [60]. This is voiced by Equation 9.

$\log q_e = \log K_f + (1/n) \log C_e$ [9]

Where K_f and n are constants integrating all factors affecting the adsorption capability that indicates the amount of adsorbate on the adsorbent and adsorption strength, respectively [61]. The value of n produces a notion about the adsorption intensity. The higher the number of n, the more uniform will be the surface and vice versa [62]. These results are presented in Fig.16

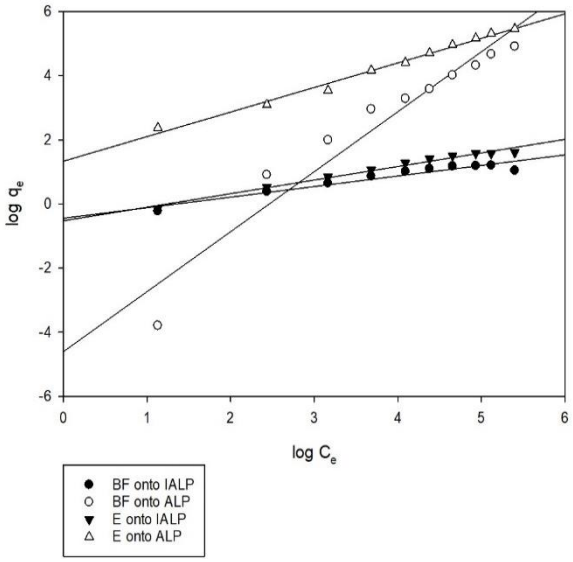

Fig. 16 Freundlich isotherm model

3.7.2.3. Temkin isotherm model

According to this isotherm model, at the covered layer there will be a linear decrease in the heat of sorption because of the leverage of interactions between sorbent and sorbate particles [63]. In addition, there will be a linear decrease in the process heat instead of logarithmic obtained from Freundlich model [64].

Temkin linear form is expressed by Equation 10

$$q_e = (RT/b_T) \ln A_T + (RT/b_T) \ln c_e \quad [10]$$

Those results are shown in Fig.17.

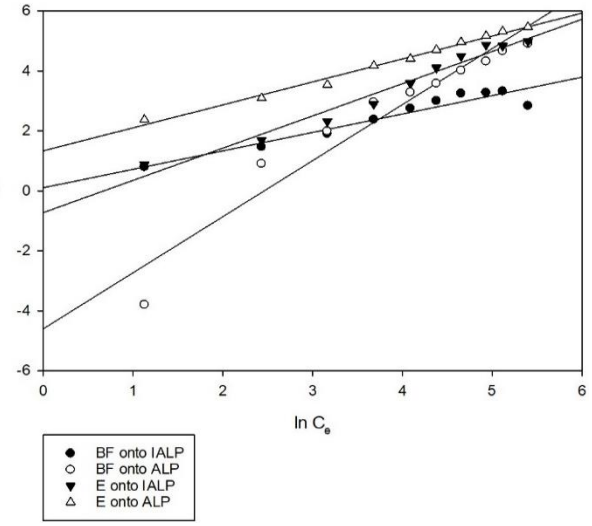

Fig. 17 Temkin isotherm model

3.7.2.4. Dubinin-Radushkevich (D-R) isotherm model

That model of isotherm was applied to adsorption for vapors on solids. This model depends on the theory of Polanyi which supposes that the distribution of pores on adsorbent surface tracks Gaussian energy distribution [65]. It is a nonlinear model which can be expressed by Equation 11

$$\ln q_e = \ln q_s - k_{DR} \varepsilon^2 \quad [11]$$

Polanyi's potential theory can be calculated from Equation 12 [66].

$$\varepsilon = RT \ln (1 + 1/C_e) \quad [12]$$

It was found that the terms ε and RT have the same dimension, so the term $(1+1/C_e)$ is meaningless since the dimensions of 1 and $1/C_e$ are inconsistent.

Now the mean free energy for each single adsorbate molecule E ($kJ \cdot mol^{-1}$) can be digitally known through Equation 13.

$$E = [1/(2K_{DR})^{1/2}] \quad [13]$$

The value of E is used to specify whether the adsorption is controlled via a physical ($E < 8$ $kJ \cdot mol^{-1}$) or a chemical process ($8 < E < 16$ $kJ \cdot mol^{-1}$) [67]. The results are presented in Fig.18.

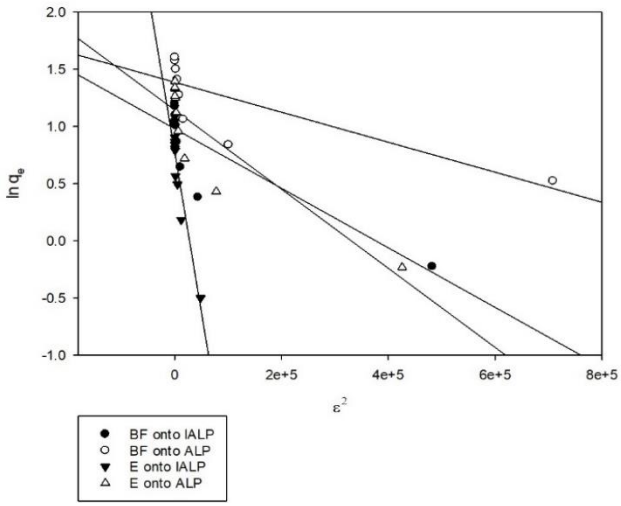

Fig. 18 Dubinin-Radushkevich (D-R) isotherm model

The parameters are calculated and compared in Table 3. The R^2 values point that the process fitted into Langmuir, Freundlich, Temkin, and Dubunin – Radushkevich isotherm models and can be best represented by Langmuir adsorption model which had the top R^2 values. So, the character of surfaces is homogeneous which supports the formation of monolayer dye particles [68]. Maximum adsorption capacities were calculated from Langmuir model to be 3.0731, 3.3190 $mg.g^{-1}$ for BF adsorption, and 3.1646, 4.0388 $mg.g^{-1}$ for E adsorption onto IALP and ALP respectively. The R_L values (ranging from 0 to 1) calculated from the Langmuir model indicate that the isotherm was favorable. The value $n > 1$ calculated from the Freundlich isotherm model suggests that the

adsorption is favorable [69]. The values of A_T and B calculated from Temkin isotherm model and the mean free energy E calculated from Dubinin-Radushkevich (D-R) isotherm model give an indication of the heat of sorption indicating a physical adsorption process [70,71].

3.7.3. Thermodynamic parameters

The temperature effect was examined and thermodynamic parameters values of the process were appraised. The thermodynamic parameters are very important because they give ideas about how the heat influences the sorption, indicating whether a certain process occurs spontaneously or not. Those parameters are the change in enthalpy (ΔH°), entropy (ΔS°), and Gibbs free energy (ΔG°) [62]. The ratio between the concentration of the compound in the aqueous medium and in solids at equilibrium was mentioned as the apparent equilibrium constant (K_c) which can be computed via Equation 14 [72].

$$k_c = \frac{c_{ad,e}}{c_e} \qquad [14]$$

In the minimum empirical adsorbate concentration, the value of K_c can be calculated [73]. Then the change in Gibbs free energy (ΔG◦) was estimated by replacing the value of K_c with Equation 15.

$$\Delta G^o = -RT \ln K_c \qquad [15]$$

Through graphing Van't Hoff equation (16), ΔH° and ΔS° were obtained.

$$\Delta G^o = \Delta H^o - T\,\Delta S^o \qquad [16]$$

ΔG^o was used to prove the spontaneity of adsorption. As the standard state is not usually reached easily, this concept of ΔG^o as an indication is limited. The basis for judgment depends on the preliminary ΔG^o value [74]. The results are presented in Fig.19. The parameters are calculated and compared in Table 4. The adsorption processes were viable and spontaneous, as a result of negative ΔG^o values [75]. The adsorption onto ALP was more favored than onto IALP and BF dye showed better results than E dye. It was found that ΔG◦ is in an inverse relationship with the temperature.

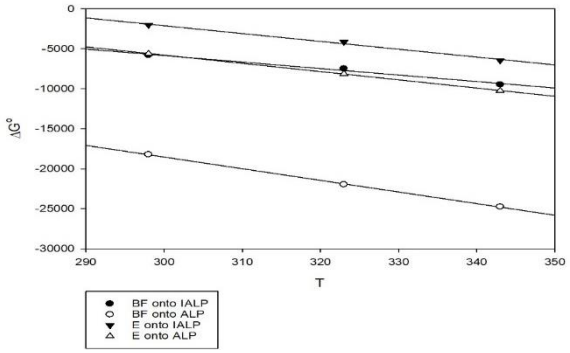

Fig. 19 Thermodynamic parameters of BF and E adsorption onto IALP and ALP.

Table 3 Isotherm parameters for BF and E dyes adsorption onto IALP & ALP

Parameter	BF onto IALP	BF onto ALP	E onto IALP	E onto ALP
Langmuir isotherm model				
b	0.1096	15.8579	0.0232	0.0729
qo	3.0731	3.3190	3.1646	4.0388
R2	0.9709	0.8239	0.9766	0.9943
RL for initial dye concentration				
35	0.0059	0.00180	0.5515	0.2815
70	0.0029	0.00090	0.3807	0.1638
100	0.0021	0.00063	0.3008	0.1206
135	0.0015	0.00047	0.2417	0.0922
170	0.0012	0.00037	0.2020	0.0746
200	0.0010	0.00032	0.1771	0.0642
235	0.0009	0.00027	0.1548	0.0551
270	0.0008	0.00023	0.1375	0.0483
300	0.0007	0.00021	0.1254	0.0437
325	0.0006	0.00019	0.1138	0.0393
Freundlich isotherm model				
Kf	0.6424	1.7269	0.3129	0.6348
n	3.0423	4.6382	2.4752	2.6137
R2	0.9193	0.9563	0.8746	0.9161
Temkin isotherm model				
B	0.6142	0.5150	0.5873	0.8181
AT	1.1855	56.981	0.3514	0.8377
bT	4.0338 x103	4.8108 x103	4.2186 x103	3.0284 x103
R2	0.9175	0.8339	0.9535	0.9428
Dubinin-Radushkevich (D-R) isotherm model				
KDR	3 x10-6	2 x10-8	3 x10-5	3 x10-6
qs	2.6666	3.5495	2.1743	3.1406
E	0.4082	5.000	0.1291	0.4082
R2	0.7380	0.6084	0.9064	0.7827

Table 4 Thermodynamic parameters for BF and E dyes adsorption onto IALP & ALP

Parameter	BF onto IALP	BF onto ALP	E onto IALP	E onto ALP
ΔGo at				
298K	-5.7841	-18.2035	-2.0118	-5.5903
323K	-7.4613	-21.9679	-4.1344	-8.1179
343K	-9.4585	-24.7515	-6.4479	-10.233
ΔHo	18.478	25.183	27.298	25.144
ΔSo	0.0811	0.1457	0.0980	0.1031
R2	0.987	0.9995	0.9921	0.9998

In other words, the adsorption processes were favored at higher temperature values. On the other hand, the adsorption was found to be endothermic with a higher randomness at the solid–solute interface, as a result of positive values of ΔH° and ΔS°, this also supports the observed increase in the adsorption capacity with increasing temperature. a notable entropy change was observed because of the low values of ΔS° [48]. The positive entropy value suggests stability, good affinity, and a decrease in the randomness of BF and E in the whole removal process [76].

4. Conclusion

Using low-cost lemon peel waste for Basic Fuchsine and Eosin dyes removal from aqueous mediums was examined in batch experiments. Lemon peel shows a higher adsorption capacity value in the activated form and the adsorption equilibrium was rapid for the adsorption process. The removal of Basic Fuchsine dye was higher than that of Eosin dye. The kinetics pursued a pseudo-second order. According to experimental data, Langmuir isotherm was the better model to characterize the adsorption processes. By increasing the temperature, adsorption increases so the adsorption processes were endothermic. An overall selectivity for both dyes was observed showing that lemon peel can be effectively used to remove Basic Fuchsine and Eosin from aqueous solutions. Thus, lemon peel is an effective and low-expensive adsorbent that can be used for the treatment of industrial wastewater especially that involving dyes.

Acknowledgments

The authors express their sincere gratitude to the Regional Center for Mycology and Biotechnology in Egypt, for the testing support of this study.

Funding

This research did not receive any specific grant from funding agencies in the public, commercial, or not-for-profit sectors.

References

1. M. Kumar, S. Ambika, A. Hassani, P.V. Nidheesh, *Waste to catalyst: Role of agricultural waste in water and wastewater treatment*. Journal of Science of The Total Environment. 858(1) (2023) 159762.
2. M. Yi-Fang, X. Gang, G. Yao-Shen, W. Bin, A. Quan-Fu, *Development of antifouling nanofiltration membrane with zwitterionic functionalized monomer for efficient dye/salt selective separation*. Journal of Membrane Science. 601 (2020) 117795.
3. O. I. Joshua, G. A. Adewale, *Adsorption of pollutants by plant bark derived adsorbents: An empirical review*. Journal of Water Process Engineering. 35 (2020) 101228.
4. A. Hashema, O. A. Chukwunonso, E. S. Abdel-Halima, A. Amr, S. Faraga, A. A. Aly, *Instrumental characteristics and acid blue 193 dye sorption properties of novel lupine seed powder*. Journal of Cleaner Chemical Engineering. 2 (2022) 100011.
5. H. M. Solayman, Md. A. Hossen, A. Abd Aziz, N. Y. Yahya, K. H. Leong, L. C. Sim, M. U. Monir, K. Zoh, *Performance evaluation of dye wastewater treatment technologies: A review*. Journal of Environmental Chemical Engineering. 11(3) (2023) 109610.
6. G. Crini, E. Lichtfouse, *Advantages and disadvantages of techniques used for wastewater treatment*. Journal of Environmental Chemistry Letters. 17 (2019) 145–155.
7. Z. Yong-Hua, G. Jin-Tao, C. Jie-Chuan, C. Yu-Fu, C. Chun-Yan, *Adsorption performance of basic fuchsin on alkali-activated diatomite*. Journal of Adsorption Science & Technology. 38(5–6) (2020) 151–167.
8. E. Plevová, S. Vallová, L. Vaculíková, M. Hundáková, R. Gabor, K. Smutná, R. Žebrák, *Organobeidellites for Removal of Anti-Inflammatory Drugs from Aqueous Solutions*. Journal of Nanomaterials. 11 (2021) 3102.
9. A. Hashem, A. A. Aly, A. M. Abdel-Mohsen, *Novel Agro-Aaste for Adsorption of Acid Violet 90 from Contaminated Water: Isotherms and Kinetics*. Journal of Research Square. (2022). https://doi.org/10.21203/rs.3.rs-1998152/v1

10. L. Bulgariu, L. B. Escudero, O. S. Bello, M. Iqbal, *The utilization of leaf-based adsorbents for dyes removal: A review*. Journal of Molecular Liquids, 276 (2018). DOI:10.1016/j.molliq.2018.12.001.
11. H. Sadegh, G. A. M. Ali, *Potential Applications of Nanomaterials in Wastewater Treatment: Nanoadsorbents Performance.* Advanced Treatment Techniques for Industrial Wastewater, (2018). DOI:10.4018/978-1-5225-5754-8.ch004
12. [12] S. Danehpash, P. Farshchi, E. Roayaei, J. Ghoddousi, A.H. Hassani, *Investigation the advantages of some biocompatible adsorbent materials in removal of environmental pollutants in aqueous solutions*. Ukrainian Journal of Ecology, 8(3) (2018) 199-202.
13. S. Moosavi, W. Lai, S. Gan, G. Zamiri, O. A. Pivehzhani, M. R. Johan, *Application of Efficient Magnetic Particles and Activated Carbon for Dye Removal from Wastewater*. Journal of American Chemical Society, 5 (2020) 20684−20697.
14. D. N. Ramutshatsha, A. Mavhungu, M. L. Moropeng, R. Mbaya, *activated carbon derived from waste orange and lemon peels for the adsorption of methyl orange and methylene blue dyes from wastewater*. Journal of Heliyon. 8 (2022) e09930.
15. S. Benkhaya, S. Mrabet, A. El Harfi, *A Review On Classifications, Recent Synthesis And Applications Of Textile Dyes, Journal Pre-proofs.* Journal of Inorganic Chemistry Communications. S1387-7003 (2020) 30058-7, INOCHE 107891.
16. M. El-Azazy, A. S. El-Shafie, A. Ashraf, A. A. Issa, *Eco-Structured Biosorptive Removal of Basic Fuchsin Using Pistachio Nutshells: A Definitive Screening Design—Based Approach*. J. Appl. Sci. 9 (2019) 4855. DOI:10.3390/app9224855.
17. A. Bukhari, I. Ijaz, H. Zain, E. Gilani, A. Nazir, A. Bukhari, S. Raza, J. ansari, S. Hussain, S. S. Alarfaji, R. saeed, Y. Naseer, R. Aftab, S. Iram, *Removal of Eosin dye from simulated media onto lemon peel-based low cost biosorbent*. Arabian Journal of Chemistry. 15 (2022) 103873.
18. S. Priya, P. D. Jason, R. Sudipta, *In situ ATR-FTIR spectroscopy for evidencing the adsorption mechanism of ammonium on a pinewood-derived biochar*. Journal of Agriculture & Environmental Letters. 8(1) (2023) 20097. https://doi.org/10.1002/ael2.20097
19. M. Kavisri, A. Marykutty, S. R. N. Karthik, J. Aravindkumar, D. Balaji, S. Ramamoorthy, S. Sivaraj, S. Ramachandran, M. Meivelu, *Adsorption isotherm, kinetics and response surface methodology optimization of cadmium (Cd) removal from aqueous solution by chitosan biopolymers from cephalopod waste.* Journal of Environ Manage. 22(335) (2023) 117484. DOI: 10.1016/j.jenvman.2023.117484
20. N. El Messaoudi, E. Abdelaziz, E. Mohammed, A. Bouich, Y. Fernine, Z. Ciğeroğlu, J. H. P. Américo-Pinheiro, N. Labjar, A. Jada, M. Sillanpää, L. Abdellah, *Experimental study and theoretical statistical modeling of acid blue 25 remediation using activated carbon from Citrus sinensis leaf*. Journal of Fluid Phase Equilibria. 563 (2022) 113585.
21. A. Aichour, H. Zaghouane-Boudiaf, C. V. Iborra, M. S. Polo, *Bioadsorbent beads prepared from activated biomass/alginate for enhanced removal of cationic dye from water medium: Kinetics, equilibrium and thermodynamic studies*. Journal of Molecular Liquids. S0167-7322 (2017) 35187-5. MOLLIQ 8715.
22. F. Hamidi, M. H. Dehghani, M. Kasraee, M. Salari, L. Shiri, A. H. Mahvi, *Acid red 18 removal from aqueous solution by nanocrystalline granular ferric hydroxide (GFH); optimization by response surface methodology & genetic-algorithm*. Journal of Scientifc Reports, 12 (2022) 4761.
23. D. Shrestha, *Removal of Eosin Y Dye using Activated Carbons from Modified Wood Dust Powder of Dalbergia sisoo*. Journal of Patan Pragya. 8(1) (2021) 2595-3278.
24. S. Zuhara, S. Pradhan, Y. Zakaria, A. R. Shetty, G. McKay, *Removal of Methylene Blue from Water Using Magnetic GTL-Derived Biosolids: Study of Adsorption Isotherms and Kinetic Models*. Journal of Molecules. 28(3) (2023) 1511. https://doi.org/10.3390/molecules28031511
25. G. Chune, G. Xiaomi, C. Wubo, J. Nan, L. He, *FTIR-ATR study for adsorption of trypsin in aqueous environment on bare and TiO2 coated ZnSe surfaces*. Journal of Chinese Chemical Letters. 31(1) (2020) 150-154. https://doi.org/10.1016/j.cclet.2019.04.067
26. M. Thirumavalavan, Y. Lai, J. Lee, *Fourier Transform Infrared Spectroscopic Analysis of Fruit Peels before and after the Adsorption of Heavy Metal Ions from Aqueous Solution*. J. Chem. Eng. 56 (2011) 2249–2255. DOI: 10.1021/je101262w.
27. H. Arslanoglu, H. S. Altundogan, F. Tumen, *Preparation of cation exchanger from lemon and sorption of divalent heavy metals*. J. Bioresource. Technol. 99 (2008) 2699–2705. DOI:10.1016/j.biortech.2007.05.022.
28. M. T. Bai, Y.V. Anudeep, C. A.I. Raju, P. V. Rao, N. Chittibabu, *Decolourization of Eosin yellow (EY) dye using a variety of brown algae*. Journal of Materials Today: Proceedings 42 (2021) 1130–1137.

29. E. Šabanović, M. Memić, J. Sulejmanović, A. Selović, *Simultaneous adsorption of heavy metals from water by novel lemon-peel based biomaterial*. Journal of Chemical Technology. 22(1) (2020) 46—53, 10.2478/pjct-2020-0007.
30. P. V. João, *On validity, physical meaning, mechanism insights and regression of adsorption kinetic models*. Journal of Molecular Liquids. 376 (2023) 121416. https://doi.org/10.1016/j.molliq.2023.121416
31. P. Anand, S. Dolly, K. Pushpak, M. Dhiraj, *Application of activated carbon in wastewater treatment.* International Journal of Engineering Applied Sciences and Technology. 3(12) (2019) 2455-2143, Pages 63-66. http://www.ijeast.com
32. M. N. Akawa, K. M. Dimpe, P. N. Nomngongo, *An adsorbent composed of alginate, polyvinyl pyrrolidone and activated carbon (AC@PVP@alginate) for ultrasound-assisted dispersive micro-solid phase extraction of nevirapine and zidovudine in environmental water samples*. J. Environ. Nanotechnol. Monit. Manag. 16 (2021) 100559.
33. A. A. E. Omodele, G. A. Adewale, O. I. Joshua, V. O. Damilola, O. A. Fisayo, *Valorisation of Cocoa (Theobroma cacao) pod husk as precursors for the production of adsorbents for water treatment*. Journal of Environmental Technology Reviews. 9(1) (2020) 20–36 https://doi.org/10.1080/21622515.2020.1730983
34. [35] F. Ahmadijokani, H. Molavi, A. Bahi, S. Wuttke, M. Kamkar, O. J. Rojas, F. Ko, M. Arjmand, *Electrospun nanofibers of chitosan/polyvinyl alcohol/UiO-66/ nanodiamond: Versatile adsorbents for wastewater remediation and organic dye removal*. Journal of Chemical Engineering. 457 (2023) 141176.
35. [34] S. Akhouairi, H. Ouachtak, A. A.Abdelaziz, A. Jada, J. Douch, *Natural Sawdust as Adsorbent for the Eriochrome Black T Dye Removal from Aqueous Solution*, Journal of Water Air Soil Pollution. (2019) 230-181. https://doi.org/10.1007/s11270-019-4234-6
36. Z. Abdul Razak, S. Rushdi, M. Y. Gadhban, S. Z. Al-Najjar, Z. T. Al-Sharify, *Possibility of Utilizing the Lemon Peels in Removing of Red Reactive (RR) Dye from Simulated Aqueous Solution.* Journal of Green Engineering (JGE). 10(10) 2020.
37. A. Peyghami, A. M., Y. Rashtbari, S. Afshin, M. Vosuoghi, D. Abdollah, *Evaluation of the efficiency of magnetized clinoptilolite zeolite with Fe3O4 nanoparticles on the removal of basic violet 16 (BV16) dye from aqueous solutions*, Journal of Dispersion Science and Technology, (2021). DOI: 10.1080/01932691.2021.1947847.
38. C. T. Tovar, Á. V. Ortíz, C. S. Ardila, M. M. Acuña, R. O. Toro, *Adsorption in a binary system of Pb (II) and Ni (II) using lemon peels. Revista Facultad de Ingeniería.* Journal of Universidad de Antioquia. 101 (2021) 31-44.
39. M. Moradi, M. A. Moradkhani, S. H. Hosseini, M. Olazar, *Intelligent modeling of photocatalytically reactive yellow 84 azo dye removal from aqueous solutions by ZnO-light expanded clay aggregate nanoparticles.* International Journal of Environmental Science and Technology,20 (2023) 3009–3022.
40. K. E. Onwuka, C. U. Aghalibe, U. T. Nkwoada, J. C. Igwe, C. E. Osigwe, K. S. Eze, *Comprehensive Review on the Efficacy of Alkylammonium Cation Pillared Clays for Sorption of Volatile Organic Carbons.* Journal of Chemistry Research. 4(6) (2019) 87-108.
41. J. Bortoluz. F. Ferrarini. L. R. Bonetto. J. S. Crespo. M. Giovanela, *Use of low-cost natural waste from the furniture industry for the removal of methylene blue by adsorption: isotherms, kinetics and thermodynamics*. Journal of Cellulose. 27 (2020) 6445–6466. https://doi.org/10.1007/s10570-020-03254-y
42. S. Bağcı, A. A. Ceyhan, *Adsorption of methylene blue onto activated carbon prepared from lupinus albus.* Journal of Chemical Industry and Chemical Engineering. 22(2) (2016) 155-165.
43. C. Johnson, *Assuring Purity of Drinking Water*. Comprehensive Water Quality and Purification, Imprint: Elsevier. (2013) eBook ISBN 978-0-12-382183-6.
44. M. A. Abdelaziz, M. E. Owda, R. E. Abouzeid, O. Alaysuy, E. I. Mohamed, *Kinetics, isotherms, and mechanism of removing cationic and anionic dyes from aqueous solutions using chitosan/magnetite/silver nanoparticles*. International Journal of Biological Macromolecules, 225 (2023) 1462-1475.
45. M. Musah, Y. Azeh, J. T. Mathew, M. T. Umar, Z. Abdulhamid, A. I. Muhammad, *Adsorption Kinetics and Isotherm Models: A Review*. Caliphate Journal of Science & Technology. CaJoST. 1 (2022) 20-26.
46. S. M. Z. Mohd, A. Muhammad, S. A. Syed, *Adsorption Isotherm and Kinetic Study of Methane on Palm Kernel Shell-Derived Activated Carbon*. Journal of Bioresources and Bioproducts. 8(1) (2023) 66-77
47. O. O. Rukayat, M. F. Usman, O. M. Elizabeth, O. O. Abosede, I. U. Faith, *Kinetic Adsorption of Heavy Metal (Copper) On Rubber (Hevea Brasiliensis) Leaf Powder*. South African Journal of Chemical Engineering. 37 (2021) 74–80.

48. F. Batool, J. Akbar, S. Iqbal, S. Noreen, S. N. A. Bukhari, *Study of Isothermal, Kinetic, and Thermodynamic Parameters for Adsorption of Cadmium: An Overview of Linear and Nonlinear Approach and Error Analysis*. Journal of Bioinorganic Chemistry and Applications. 11 (2018). Article ID 3463724.
49. A. N. Ebelegi, N. Ayawei, D. Wankasi, *Interpretation of Adsorption Thermodynamics and Kinetics*. Journal of Physical Chemistry. 10 (2020) 166-182.
50. A. A. Akram, D. Axelle, M. Mohanned, M. B. Anne, M. Nader, *CO_2 capture using in-situ polymerized amines into pore-expanded-SBA-15: Performance evaluation, kinetics, and adsorption isotherms*. Journal of Fuel. 333(1) (2023) 126401. https://doi.org/10.1016/j.fuel.2022.126401
51. R. A. Lina, P. Le Coustumer, R. G. Stéphan, Z. Stéphane, S. Serge, *Removal efficiency and adsorption mechanisms of CeO2 nanoparticles onto granular activated carbon used in drinking water treatment plants*. Journal of Science of The Total Environment. 856(2) (2023) 159261. https://doi.org/10.1016/j.scitotenv.2022.159261
52. G. M. Neelgund, S. F. Aguilar, E. A. Jimenez, R. L. Ray, *Adsorption Efficiency and Photocatalytic Activity of Silver Sulfide Nanoparticles Deposited on Carbon Nanotubes*. Journal of Catalysts. 13 (2023) 476.https://doi.org/10.3390/catal13030476.
53. I. Ghosh, S. Kar, T. Chatterjee, N. Bar, S. K. Das, *Removal of methylene blue from aqueous solution using Lathyrus sativus husk: adsorption study, MPL and ANN modelling*. Journal of Pre-proof. S0957-5820 (2920) 31861-9. PSEP 2568.
54. [54] M. Khnifira, W. Boumya, J. Attarki, A. Mahsoune, M. Abdennouri, M. Sadiq, S. Kaya, N. Barka, *Adsorption characteristics of dopamine by activated carbon: Experimental and theoretical approach*. Journal of Molecular Structure. 1278 (2023) 134964. https://doi.org/10.1016/j.molstruc.2023.134964
55. M. T. Alotaibi, Roaa T. Mogharbel, A. Q. Alorabi, N. A. Alamrani, S.Ahmed , N. M. El-Metwaly, *Superior adsorption and removal of toxic industrial dyes using cubic Pm3n aluminosilica form an aqueous solution, Isotherm, Kinetic, thermodynamic and mechanism of interaction*. Journal of Molecular Liquids 379 (2023) 121672.
56. X. Liu, H. Lu, Q. Li, Z. Fu, F. Tan, X. Wang, J. Zhou, *Magnetic molecularly imprinted polymers for selectively adsorbing flavins and their effects on bioremoval of Acid Red 18 and Cr(VI)*. Journal of Chem. Technol. Biotechnol. 97(8) (2022) 2047–2054.
57. M. Rajabi, S. Keihankhadiv, Suhas et al. *Comparison and interpretation of isotherm models for the adsorption of dyes, proteins, antibiotics, pesticides and heavy metal ions on different nanomaterials and non-nano materials-a comprehensive review*. Journal of Nano struct. Chem. 13 (2023) 43-65. https://doi.org/10.1007/s40097-022-00509-x
58. G. K. Rajahmundry, C. Garlapati, P. S. Kumar, R. S. Alwi, N. V. Dai-Viet, *Statistical analysis of adsorption isotherm models and its appropriate selection*. Journal of Chemosphere. 276 (2021) 130176.
59. S. S. Shah, T. Sharma, B. A. Dar, R. K. Bamezai, *Adsorptive removal of methyl orange dye from aqueous solution using populous leaves: Insights from kinetics, thermodynamics and computational studies*. Journal of Environmental Chemistry and Ecotoxicology. 3 (2021) 172–181.
60. A. A. Mohammad, D. A. Da'ana, *Guidelines for the use and interpretation of adsorption isotherm models: A review*. Journal of Hazardous Materials. 393 (2020) 122383.
61. H. Qili, L. Rui, H. Liru, L. Hengyuan, P. Xiangjun, *A critical review of adsorption isotherm models for aqueous contaminants: Curve characteristics, site energy distribution and common controversies*. Journal of Environmental Management. 329(1) (2023) 117104.
62. C. Estrada, A. Karen, C. Lozano, Felipe, L. Díaz, R. Alejandro, *Thermodynamics and Kinetic Studies for the Adsorption Process of Methyl Orange by Magnetic Activated Carbons*. Journal of Bio One Complete. 14 (2021) 1–11. https://doi.org/10.1177/11786221211013336
63. K. Alok, S. Sumati, K. Balasubramanian, *A review on algal biosorbents for heavy metal remediation with different adsorption isotherm models*. Journal of Environmental Science and Pollution Research. 30(4) (2023) 1-20. https://doi.org/10.1007/s11356-023-25710-5
64. C. A. Riyanto, E. Prabalaras, *The adsorption kinetics and isoterm of activated carbon from Water Hyacinth Leaves (Eichhornia crassipes) on Co(II)*. International Conference on Science and Science Education, Journal of Physics: Conf. Series 1307 (2019) 012002.
65. J. Wang, X. Guo, *Adsorption isotherm models: Classification, physical meaning, application and solving method*. Journal Pre-proof, Chemosphere. S0045-6535(2920)31472-7. CHEM 127279.
66. P. Chidamparam, M. J. Rajamani, M. Jayabalakrishnan, P. Mohan, B. Govindaraj, L. Arunachalam, S. Selvakumar, Z. J. Joseph, *Cellulose-based hydrogel for adsorptive removal of cationic dyes from aqueous solution: isotherms*

and kinetics. Journal of RSC Advances. 13 (2023) 4757-4774. DOI: 10.1039/d2ra08283g

67. C. H. Pimentel · M. S. Freire, D. G. Díaz, J. G. Álvarez, *Removal of wood dyes from aqueous solutions by sorption on untreated pine (Pinus radiata) sawdust*. Journal of Cellulose. 30 (2023) 4587–4608. https://doi.org/10.1007/s10570-023-05145-4
68. H. Ouachtak, A. El Guerdaoui, R. Haounati, S. Akhouairi, R. ElHaouti, N. Hafid, A.Abdelaziz, B. Šljukić, D. M. F. Santos, M. L. Taha, *Highly efficient and fast batch adsorption of orange G dye from polluted water using superb organo-montmorillonite: Experimental study and molecular dynamics investigation*. Journal of Molecular Liquids. 335 (2021) 116560.
69. A. N. Alene, G. Y. Abate, A. T. Habte, D. M. Getahun, *Utilization of a Novel Low-Cost Gibto (Lupinus Albus) Seed Peel Waste for the Removal of Malachite Green Dye: Equilibrium, Kinetic, and Thermodynamic Studies*. Journal of Chemistry. 16 (2021) 6618510. https://doi.org/10.1155/2021/6618510
70. A. O. Dada, A. P. Olalekan, A. M. Olatunya, O. Dada, *Langmuir, Freundlich, Temkin and Dubinin–Radushkevich Isotherms Studies of Equilibrium Sorption of Zn2+ Unto Phosphoric Acid Modified Rice Husk*. Journal of Applied Chemistry (IOSR-JAC). 3(1) (2012) 2278-5736. PP 38-45.
71. N. Ayawei, A. N. Ebelegi, D. Wankasi, *Modelling and Interpretation of Adsorption Isotherms*. Journal of Chemistry. 11 (2017) 3039817. DOI:10.1155/2017/3039817.
72. M. A. Ahmed, M. A. Ahmed, A. A. Mohamed, *Synthesis, characterization and application of chitosan/graphene oxide/copper ferrite nanocomposite for the adsorptive removal of anionic and cationic dyes from wastewater*. Journal of Royal Society of Chemistry. 13 (2023) 5337–5352.
73. R. Hana, J. Zhanga, P. Hana, Y. Wanga, Z. Zhao, M. Tanga, *Study of equilibrium, kinetic and thermodynamic parameters about methylene blue adsorption onto natural zeolite*. Journal of Chemical Engineering. 145 (2009) 496–504.
74. T. Chen, T. Da, Y. Ma, *Reasonable calculation of the thermodynamic parameters from adsorption equilibrium constant*. Journal of Molecular Liquids 322 (2021) 114980.
75. M. N. Sahmoune, *Evaluation of thermodynamic parameters for adsorption of heavy metals by green adsorbents*. Journal of Environmental Chemistry Letters. 17 (2019) 697–704.
76. H. Boulika, M. El Hajam, M. H. Nabih, I. R. Karim, N. I. Kandri, A. Zerouale, *Definitive screening design applied to cationic & anionic adsorption dyes on Almond shells activated carbon: Isotherm, kinetic and thermodynamic studies*. Journal of Materials today : Proceedings 72 (7) (2023) 3336-3346.